HHS Public Access

Author manuscript

Nat Commun. Author manuscript; available in PMC 2015 July 09.

Published in final edited form as:

Nat Commun. ; 6: 5914. doi:10.1038/ncomms6914.

Vasculopathy associated hyperangiotensinemia mobilizes hematopoietic stem cells/progenitors through endothelial AT_2R and cytoskeletal dysregulation

Kyung Hee Chang[1,2], **Ramesh C. Nayak**[2], **Swarnava Roy**[2], **Ajay Perumbeti**[1], **Ashley M. Wellendorf**[2], **Katie Y. Bezold**[2], **Megan Pirman**[1], **Sarah E. Hill**[1], **Joseph Starnes**[2], **Anastacia Loberg**[2], **Xuan Zhou**[2], **Tadashi Inagami**[3], **Yi Zheng**[2], **Punam Malik**[2,*], and **Jose A. Cancelas**[1,2,*]

[1]Hoxworth Blood Center, University of Cincinnati College of Medicine, 3130 Highland Avenue, Cincinnati, OH 45267, USA

[2]Division of Experimental Hematology, Cincinnati Children's Research Foundation, Cincinnati Children's Hospital Medical Center, 3333 Burnet Avenue, Cincinnati, OH 45229, USA

[3]Vanderbilt University School of Medicine, 1161 21st Ave S., Nashville, TN 37232

Abstract

Patients in organ failure of vascular origin have increased circulating hematopoietic stem cells and progenitors (HSC/P). Plasma levels of angiotensin II (Ang-II), are commonly increased in vasculopathies. Hyperangiotensinemia results in activation of a very distinct Ang-II receptor set, Rho-family GTPase members, and actin in bone marrow endothelial cells (BMEC) and HSC/P, which results in decreased membrane integrin activation in both BMEC and HSC/P, and in HSC/P de-adhesion and mobilization. The Ang-II effect can be reversed pharmacologically and genetically by inhibiting Ang-II production or signaling through BMEC AT2R, HSCP AT_1R/AT_2R or HSC/P RhoA, but not by interfering with other vascular tone mediators. Hyperangiotensinemia and high counts of circulating HSC/P seen in sickle cell disease (SCD) as a result of vascular damage, is significantly decreased by Ang-II inhibitors. Our data define for the first time the role of Ang-II HSC/P traffic regulation and redefine the hematopoietic consequences of anti-angiotensin therapy in SCD.

*To whom correspondence should be addressed: Jose A. Cancelas, MD, PhD & Punam Malik, MD, Division of Experimental Hematology and Cancer Biology, Cincinnati Children's Hospital Medical Center, 3333 Burnet Ave., Cincinnati, OH, 45229, USA, Tel: +1-513-803-0939; Fax: +1-513-558-1522, jose.cancelas@cchmc.org; punam.malik@cchmc.org.

Supplementary Information accompanies this manuscript.

Author contributions

KHC, YZ, PM and JAC designed experiments. KHC, RN, SR, AP, AMF, KB, MP, SEH, AL and XZ performed experiments. PM, YZ and TI contributed new reagents/analytic tools. KHC, RN, AP, PM and JAC analyzed data. KHC, PM and JAC wrote the manuscript.

Competing Financial Interest Statement

The authors declare filing of intellectual property protection.

Keywords

Angiotensin II; hematopoietic stem cell/progenitor; mobilization connexin-43; integrin; Rho GTPases

Introduction

Hematopoietic stem and progenitor cells (HSC/P) are needed constantly to replace mature blood cells. The bone marrow (BM) microenvironment regulates a homeostatic dynamic equilibrium with a pool of circulating HSC/P[1–5]. The size of the circulating pool of HSC/P is critically regulated by their adhesion or de-adhesion to their microenvironment. Patients in organ failure of vasculo-endothelial origin have an increased circulating pool of HSC/P[6–8] and which may represent a homeostatic stress response contributing to vascular damage repair[9]. An example of systemic vasculo-endothelial disease is sickle cell disease (SCD) which is associated with endothelial activation and damage[10] and an increased pool of circulating primitive hematopoietic progenitors[11].

Angiotensin II (Ang-II) is the major bioactive peptide of the renin-angiotensin system and is implicated in homeostatic regulation of blood volume, vascular tone and sodium retention[12]. Patients with vascular disease commonly develop secondary hyperangiotensinemia and BM dysfunction of multifactorial origin [13]. There is evidence for the effect of Ang-II in hematopoiesis. Studies have shown that animals and patients receiving Ang-II targeted therapies had decreased stress erythropoiesis[14–18], suggesting the existence of a local Ang-II regulatory system in the BM that is involved in the regulation of hematopoiesis[19]. However, the intrinsic or extrinsic nature of the mechanisms by which Ang-II regulates HSC/P activity in pathological conditions remains unknown.

In this study, we reveal that acute and chronic hyperangiotensinemia in mice results in an increased pool of circulatory HSC/P, which can be reversed pharmacologically or genetically by a microenvironmental deficiency of angiotensin II receptor type 2 (AT_2R). Hyperangiotensinemia results in HSC/P de-adhesion from BM endothelial cells (BMEC) through distinct changes in the balance of the activated Rho family GTPases, Rho and Rac, and in cytoskeletal rearrangements in the BMEC and HSC/P. We show that untreated patients with SCD have high levels of blood Ang-II and HSC/P in circulation, which significantly decreases upon angiotensin-targeted pharmacological or genetic intervention. These results indicate a new role for angiotensin in HSC/P trafficking under pathological conditions, and define the hematopoietic consequences of anti-antigiotensin therapy in SCD.

Results

Hyperangiotensinemia increases the pool of circulating HSC/P

In order to understand whether hyperangiotensinemia results in increased mobilization of HSC/P, we first used a murine model of chronic hyperangiotensinemia secondary to a vasculopathy. An endothelial cell (EC) deficiency of *Cx43*, a gap junction forming protein that is crucial in maintaining EC-to-EC junctions and preserving the barrier function of EC, has been shown to result in chronic effective hypovolemia, hypotension, and secondary

hyperreninemic hyperangiotensinemia[20]. We have generated independently endothelial *Cx43* deficient mice by crossing Tie2-Cre expressing mice with biallelic *Cx43* exon 2 floxed mice, demonstrated that these mice lack expression of Cx43 in BMEC and recombined the *Cx43* gene in colonies derived from peripheral blood while still expressed Cx43 in BM stromal cells (Supplementary Figure 1a–b). We have named these mice HyperAng-II$^{\Delta Cx43\text{-}EC}$ mice to summarize this dual property of deletion of *Cx43* in EC and hyperangiotensinemia. HyperAng-II$^{\Delta Cx43\text{-}EC}$ mice had normal numbers of peripheral blood (PB) leukocyte subpopulations (Supplementary Fig. 1c–f), blood hemoglobin, and erythrocyte and platelet counts (Supplementary Fig. 1g–i), but had a 2–3 fold increase in the number of circulating myeloid committed hematopoietic progenitors (Fig. 1a) and repopulating stem cells (Fig. 1b) compared to their wild type (WT) control littermates. Immunophenotypic enumeration of circulating HSC/P in HyperAng-II$^{\Delta Cx43\text{-}EC}$ mice indicated that both the HSC and different populations of committed progenitors, including long-term HSC (LT-HSC), short-term HSC (ST-HSC), multipotential progenitors (MPP), common myeloid progenitors (CMP), granulo-macrophagic progenitors (GMP) and megakaryoblastic-erythroid progenitors (MEP), were consistently increased 2–3 fold(Supplementary Fig. 2a–e). The increase in circulating HSC/P accounts for ~0.1% competitive repopulating units (CRU) and ~0.5% colony forming units (CFU)-C, respectively, of all BM HSC/P. These levels are similar to the mobilization with the CXCR4 inhibitor, AMD3100 [21]. As expected, the BM content of immunophenotypically defined HSC/P (Supplementary Fig. 2f–g) as well as functional progenitors (Fig. 1c) and competitive repopulating stem cells (Fig. 1d) were not significantly different in HyperAng-II$^{\Delta Cx43\text{-}EC}$ mice compared with their WT control littermates, which explains the apparent absence of changes in the content of HSC/P in the BM. Similar to BM, there was no significant changes in the splenic content of HSC/P in the HyperAng-II$^{\Delta Cx43\text{-}EC}$ mice (Fig. 1e). Interestingly, the deficiency of Cx43 in HSC/P alone does not induce HSC/P mobilization[22,23], suggesting the existence of a non-cell autonomous effect of Cx43 deficiency in HyperAng-II$^{\Delta Cx43\text{-}EC}$ mice. Generation of chimeric animals with normal hematopoiesis and Tie2-Cre;Cx43-deficient microenvironment (Fig. 1f) phenocopied the increased level of circulating HSC/P, confirming that the increase in circulating HSC/P in HyperAng-II$^{\Delta Cx43\text{-}EC}$ mice was of non-cell autonomous origin (Fig. 1g). The increased number of circulating HSC/P in these mice was not associated with increased circulating levels of the chemokines Cxcl12 (Supplementary Fig. 2h) or stem cell factor (Scf) (Supplementary Fig. 2i), which are expressed by BMEC and BM stromal cells, and are reported to function as major regulators of HSC/P content and trafficking [2,3]. β-adrenergic stimulation has also been shown to be critical at controlling HSC/P egress [24]. We did not observe any significant changes in the levels of norepinephrine or epinephrine in the BM (Supplementary Fig. 2j–k) or blood (Supplementary Fig. 2l–m) of HyperAng-II$^{\Delta Cx43\text{-}EC}$ mice, nor did the β-adrenergic blocker propranolol have an effect on their circulating HSC/P counts (Supplementary Fig. 2n). To demonstrate whether the increased level of Ang-II was responsible for the increased circulation of HSC/P, HyperAng-II$^{\Delta Cx43\text{-}EC}$ mice were given the angiotensin-converting-enzyme (ACE) inhibitor enalapril, which blocks the transformation of Ang-I into Ang-II. Enalapril was effective in reducing the plasma levels of Ang-II in HyperAng-II$^{\Delta Cx43\text{-}EC}$ mice and restored the increased count of circulating/

mobilized HSC/P to levels similar to control animals (Fig. 1h–i), indicating that the ACE-mediated formation of Ang-II is implicated in the mobilization of HSC/P to the PB.

HSC/P mobilization by Ang-II cannot be reversed by hydralazine

We then analyzed whether the HSC/P mobilization required chronic exposure to high levels of Ang-II or whether it could be achieved by transient hyperangiotensinemia as a result of a bolus administration of Ang-II. WT mice were administered 1.44 mg/Kg Ang-II dissolved in isotonic phosphate buffered saline (PBS) intraperitoneally, which resulted in increased plasma levels of Ang-II at 1, 5 and 15 minutes after administration, returning to basal levels by 30 minutes after infusion (Supplementary Fig. 2o). The administration of Ang-II resulted in significantly increased circulation of HSC/P in PB within 15 minutes post-infusion, which returned to basal levels by 30 minutes post-infusion (Fig. 2a). Furthermore, continuous infusion of Ang-II reaching an ~3-fold increase of plasma Ang-II levels over the endogenous production (Supplementary Fig. 2p) and resulted in concomitant increased counts of circulating HSC/P (Figs. 2b and **S2q**). Together, this data indicated the existence of a temporal relationship between the administration of Ang-II and HSC/P mobilization to the PB of normal mice.

To discern whether the effect of hyperangiotensinemia is associated with its vasopressor effects, we performed experiments where we combined the infusion of Ang-II with pharmacological doses of hydralazine, a vasorelaxant with activity independent of Ang-II signaling[25]. When used at doses demonstrated to reduce blood pressure in mice (1–5 mg per Kg)[26] and able to counteract the vasopressor effects of Ang-II[27], the hydralazine pre-treatment did not significantly affect the plasma levels of exogenous Ang-II (Supplementary Fig. 3a), and the vasorelaxant effect of 1 mg perKg hydralazine did not reverse the HSC/P mobilizing effect of Ang-II (Supplementary Fig. 3b), suggesting that the vasoconstriction effect of Ang-II was not responsible for the effect on HSC/P mobilization. This data, along with the rapid *in vivo* effect of the exogenous administration of Ang-II, suggest a direct effect of the hormone on Ang-II receptors.

Ang-II effects through distinct AT receptors in HSC/P and BMEC

Two distinct Ang-II receptor subtypes, AT_1R and AT_2R, which have been identified on the basis of their differential pharmacological and biochemical properties induce specific signaling pathways and seem to play distinct and sometimes opposite roles in vascular regulation [28]. Both AT_1R and AT_2R are expressed by BMEC and HSC/P (Supplementary Fig. 3c). In order to elucidate whether AT_1R or AT_2R were specifically responsible for the HSC/P mobilization phenotype, we evaluated the level of HSC/P mobilization after Ang-II administration in models of loss of function of Ang-II receptors. $AT_1R^{-/-}$ and $AT_2R^{-/-}$ mice were given a single dose of Ang-II and the level of circulating HSC/P was analyzed. While the deficiency of AT_1R did not modify the effect of Ang-II on HSC/P mobilization, the single deficiency of AT_2R completely prevented the increased HSC/P mobilization response after pharmacological administration of Ang-II (Fig. 2c), or in our model of chronic hyperangiotensinemia with AT_2R deficiency (Fig. 2d), indicating that AT_2R is indispensable to mediate the mobilization of HSC/P induced by Ang-II.

To examine whether Ang-II/AT_2R activity was cell autonomous or not, and whether the expression of other murine AT_1R subtypes [29] may have been overlooked in our genetic murine model of AT_1R deficiency, we generated chimeric animals by transplanting BM HSC/P from CD45.2$^+$ WT and CD45.2$^+$ *$AT_2R^{-/-}$* mice into myeloablated B6.SJL$^{Ptprca\ Pepcb/BoyJ}$ CD45.1$^+$ recipient mice (WT and *H-$AT_2R^{-/-}$*, respectively). Conversely, we also generated the chimeric mice with transplantation of BM HSC/P from congenic WT CD45.1$^+$ mice into CD45.2$^+$ *$AT_2R^{-/-}$* mice (*HM- $AT_2R^{-/-}$*). At 6 weeks post-transplantation, fully chimeric mice (as assessed by flow cytometry) were analyzed for the effect of the genetic deficiency of *AT_2R* in both hematopoietic and microenvironment compartments and for pharmacological inhibition of all AT_1R forms (AT_1Ra and AT_1Rb) on progenitor mobilizing response to Ang-II at 15 minutes post-administration (Fig. 2e). The single deficiency of AT_2R in the hematopoietic microenvironment prevented Ang-II-mediated HSC/P mobilization (Fig. 2f), demonstrating that a non-cell autonomous effect suffices to induce Ang-II/AT_2R dependent HSC/P mobilization. The deficiency of AT_2R expression in the hematopoiesis of chimeric animals within a WT microenvironment, or the administration of the AT_1R inhibitor, losartan, to chimeric WT mice did not prevent Ang-II-mediated mobilization of HSC/P, demonstrating that hematopoietic AT_2R or pharmacological blockade of all forms of AT_1R did not reverse the HSC/P mobilizing effect of Ang-II. However, the the combination of a genetic deficiency of HSC/P *AT_2R* and the specific pharmacological blockade of AT_1R with losartan in chimeric mice prevented the HSC/P mobilizing effect of Ang-II (Fig. 2f) indicating the presence of a hematopoietic intrinsic effect on Ang-II dependent HSC/P mobilization which can only be prevented by a combined blockade of both AT_1R and AT_2R.

AT_2R activation induces HSC/P mobilization

Pharmacological administration of the AT_2R agonist C21[30], which specifically binds to and activates AT_2R but has different pharmacokinetic and pharmacodynamic temporal activity from Ang-II [31], phenocopied the effect of Ang-II on the mobilization of hematopoietic progenitors (Fig. 2g and Supplementary Fig. 3d) and HSC (Fig. 2h and Supplementary Fig. 3e) by 4 hours after administration. Administration of C21 did not modify endogenous levels of Ang-II (Supplementary Fig. 3f) and its effect was prevented by deficiency of AT_2R (Supplementary Fig. 3g), indicating that C21 acted through an on-target effect.

To identify whether Ang-II and the clinically used HSC/P mobilizer agent G-CSF collaborate *in vivo*, we treated C57Bl/6 mice with G-CSF (200 $\mu g^{-1}Kg^{-1}$day) for 5 days followed by a single injection of the AT_2R agonist C21, and determined their effect on the blood content of HSC/P using competitive repopulation and colony forming cell assays at 4 hours after the administration of C21 on the 5th day of G-CSF administration. As shown in Supplementary Fig. 3h–i, no additive or negative effect was observed by the combination of G-CSF in either assay, which strongly suggested that both G-CSF and Ang-II act through common signaling pathways. These data are in line with previous observations in mice where inhibition of Rac GTPase activity resulted in mobilization of HSC/P, but no additional effect of G-CSF on HSC/P mobilization was found[32,33].

Ang-II dependent HSC/P mobilization is not mediated by nitric oxide (NO)

HyperAng-II$^{\Delta Cx43\text{-}EC}$ mice have been shown to have increased plasma levels of NO [20] and Ang-II has been shown to induce NO release from EC[34]. NO levels also affect endothelial function [35] and HSC release from endothelial niches [36]. To determine whether the regulation of NO levels in HyperAng-II$^{\Delta Cx43\text{-}EC}$ mice is implicated in HSC/P mobilization, we first analyzed and confirmed the presence of increased activation levels of nitric endothelial oxide synthase (eNOS) in *ex-vivo* propagated BM CD45^{-}Ter119^{-}CD31^{+}CD106^{+} BMEC from WT and HyperAng-II$^{\Delta Cx43\text{-}EC}$ mice (Supplementary Fig. 3j). Then, we analyzed whether the exogenous administration of pharmacological doses of Ang-II or the NO scavenger, L-NG-nitroarginine methyl ester (L-NAME), to WT C57Bl/6 mice, resulted in changes in the levels of nitrates/nitrites and HSC/P in blood. Administration of either Ang-II or L-NAME reduced the plasma levels of nitrates/nitrites (Supplementary Fig. 3k) but L-NAME did not modify the circulating counts of HSC/P (Supplementary Fig. 3l). Similarly, the administration of the NO donor, S-nitroso-N- acetylpenicillamine (SNAP), to WT C57Bl/6 mice did not result in changes in the count of PB HSC/P (Supplementary Fig. 3m). Altogether, this data indicates that plasma NO levels do not mediate Ang-II dependent HSC/P mobilization.

Ang-II induces HSC/P de-adhesion from BMEC

Adhesion of HSC/P to the endothelial microenvironment is a basic mechanism of retention and homing of HSC/P within the BM that fits the response-time associated with the rapid effect of the administration of Ang-II. BMEC and BM stromal cells of mesenchymal origin have been reported to tightly control BM homing and/or retention of HSC/P [3,37]. To understand whether the HSC/P adhesion to the endothelial microenvironment was impaired in the presence of Ang-II, we first analyzed if Ang-II modifies the adhesion of HSC/P to BMEC. When BMEC-adhered HSC/P were exposed to Ang-II at a concentration similar to the peak plasma level reached after the single-dose intraperitoneal administration, the fraction of BMEC-adherent HSC/P was significantly reduced (Fig. 2i). Confirming the independence of the effect of Ang-II on Cx43 expression, a comparable level of HSC/P de-adhesion was noticed when BMEC from either WT or HyperAng-II$^{\Delta Cx43\text{-}EC}$ mice were used (Fig. 2i). Interestingly, the adhesion of HSC/P to murine BM stromal cells was not reduced when cultures were exposed to Ang-II (Figure 2i), suggesting that Ang-II has a specific effect on the adhesion of HSC/P to BMEC.

Ang-II induces opposite effects on actin polymerization of HSC/P versus BMEC

Migration of HSC/P out of their tissue niches requires the disruption of cellular ligand-receptor adhesion molecules and/or the development of major destabilizing cytoskeletal rearrangements. Major molecular endothelial mediators of adhesion and HSC activity in the BM vascular niche are VCAM-1 [38] and E-selectin [39], which have been shown to be regulated by Ang-II in other cell types [40]. Ang-II did not induce significant changes in the expression level of VCAM-1 (Supplementary Fig. 3n) or E-selectin (CD62e, Supplementary Fig. 3o) on the membrane of BMEC followed for up to 15 minutes. In addition, cell adhesion is regulated by the dynamic reorganization of actin as well as the microtubule cytoskeleton. This involves cycles of net assembly and disassembly of actin filaments. Ang-

II receptors are G protein-coupled receptors with signaling activity that induces cytoskeletal reorganization through cell-context dependent activation or inhibition of members of the Rho family of small GTPases [41,42]. Therefore, we first analyzed F-actin polymerization upon Ang-II stimulation of BMEC. Confocal microscopy analysis confirmed reduced focal adhesion and stress fibers, redistribution of cortical F-actin, and significant morphological changes in BMEC after Ang-II exposure (Supplementary Fig. 4a–b). F-actin location redistributed from stress fibers to the subcortical region at 5 minutes after Ang-II treatment (Supplementary Fig. 4b). Pharmacological inhibition of Ang-II signaling using specific blockers against AT_1R (losartan) or AT_2R (PD123319) demonstrated that Ang-II-AT_2R signaling in BMEC is responsible for BMEC cytoskeletal rearrangements involving cortical actin condensation, and shape changes that reduce BMEC width (Fig. 3a–c). Interestingly, the blockade of Ang-II-AT_1R signaling enhanced changes in cell morphology, further reducing cell width, and increased cortical actin condensation (Fig. 3a–c) which may be due to the increased availability of Ang-II to bind AT_2R. Reorganization of polymerized actin correlated with decreased Rac activation (Fig. 3d), increased Rho activation (Fig. 3e) and increased inactivation through phosphorylation of cofilin (Supplementary Fig. 4c), an actin-binding protein that depolymerizes actin filaments and depends on Rac/PAK/LIMK1 activity. Altogether, this data indicate that Ang-II induces AT_2R dependent Rac inhibition and Rho activation in BMEC which results in significant cytoskeletal rearrangements and cell contraction.

Ang-II activates different Rho family of GTPases in HSC/P versus BMEC

In lung cancer bearing mice, chronic cell-autonomous Ang-II/AT_1R signaling has been shown to amplify the splenic content of HSC/P and macrophage progenitors[43]. To analyze the cellular mechanism of rapid HSC/P de-adhesion from BMEC, we designed co-cultures of HSC/P with WT BMEC and analyzed the level of actin polymerization in HSC/P after the addition of Ang-II. As source of HSC/P, BM LK cells were used and allowed to adhere onto WT BMEC in the same fashion as in Fig. 2i, and analyzed at different time points after Ang-II addition. Confocal microscopy of these co-cultures revealed reduced cortical localization of polymerized actin and an overall ~20% reduction in F-actin clustering in BM LK cells, as early as 5 minutes after Ang-II stimulation (Supplementary Fig. 4d–e), which closely preceded HSC/P de-adhesion *in vitro* and mobilization *in vivo* (as shown in Fig. 2i and 2a, respectively). Co-cultures of BM LK cells with BMEC demonstrated that the decrease in cortical actin polymerization of HSC/P required both AT_2R and AT_1R cell-autonomous signaling (Fig. 3f–g), suggesting that Ang-II signals through both AT_2R and AT_1R in HSC/P in order to disrupt the cytoskeletal integrity of adhered cells. Effector pull-down assays of Rho from isolated, adhered HSC/P, indicated that the activation of Rho in HSC/P was significantly decreased at 5 minutes after Ang-II stimulation (Fig. 3h), mirror imaging the Rho GTPase activation signaling of BMEC upon Ang-II stimulation. Cytoskeletal and Rho activity changes were associated with activation of Rac and inhibition of myosin light chain activation (Supplementary Fig. 4f–g). Phenocopying the loss of RhoA induced by Ang-II, genetic deletion of HSC/P *RhoA* activity in an inducible murine model (Supplementary Fig. 4h) resulted in HSC/P mobilization at levels similar to those of HyperAng-II$^{\Delta Cx43\text{-}EC}$ mice which was unresponsive to exogenous administration of Ang-II (Fig. 3i). This data strongly suggested that HSC/P Rho activity is required for Ang-II

dependent cell-autonomous HSC/P mobilization, and that the activation of HSC/P Rho signaling is dependent on both AT_1R and AT_2R.

Ang-II decreases expression of activated β1-integrin on the membrane of HSC/P and BMEC

Impaired activation of β1-integrins is dependent on a fine regulation of Rho family GTPase activity [44] and has been shown to be crucial for HSC/P adhesion to the BM microenvironment [45]. Cytoskeletal and Rho/Rac activity changes induced by Ang-II were not associated with changes in the expression or localization of membrane BMEC or HSC/P β1-integrin (Supplementary Fig. 4i–l) but did impair membrane β1-integrin activation in BMEC (~65% inhibition, Fig. 3j and 3l) and more modestly in HSC/P (~10% inhibition, Fig. 3k and 3m). Overall, this data indicates that Ang-II induces cytoskeletal dysregulation in both BMEC and HSC/P in synchronous, mirror image processes of Rho family members. Similar to other cell types [46,47], the in-vivo loss of Rac or Rho activity results in decreased membrane activated membrane β1-integrin expression resulting in HSC/P-BMEC de-coupling and de-adhesion, suggesting that this is a highly conserved mechanism of cell adhesion.

Hyperangiotensinemia is a major mechanism of HSC/P mobilization in SCD

SCD results from substitution of a single nucleotide, valine for glutamic acid, at the sixth amino acid of the β-globin chain of hemoglobin A. SCD is characterized by globin polymerization that results in red cell dehydration, hemolysis, and subsequent stress erythropoiesis. Vascular occlusions and pathology is a common feature in SCD patients [10]. There is also an increased circulatory count of primitive HSC/P in SCD patients [11]. The mechanism of endogenous mobilization of HSC/P in SCD patients has not yet been delineated, however, it has been speculated that they may be a by-product of local inflammatory responses to the underlying vasculopathy prevalent in many organ sites in SCD patients [11]. Based on the known pathobiological effects of SCD on endothelial function and our data regarding the role of Ang-II in HSC/P mobilization, we hypothesized that the increased circulation of HSC/P in SCD may be secondary to hyperangiotensinemia. To test this hypothesis, we analyzed PB specimens from SCD animals and patients. Berkeley sickle cell mice (Berk-SS) are used as animal models of human SCD, and exclusively express the human globins, human *α- and β^S-globin*, with deletions of the murine *α- and β-globin* genes [48]. These mice recapitulate all the features found in humans with SCD, including irreversibly sickled red cells, anemia and vasculopathy. Compared to WT mice (either Berk-AA or C57Bl/6 mice), Berk-SS mice had increased levels of Ang-II (Fig. 4a), which correlated with increased numbers of circulating HSC/P (Fig. 4b–c and Supplementary Figs. 5a–d). A group of WT mice that had been transplanted with the BM of Berk-SS mice, also showed a significantly increased level of Ang-II compared to the WT cohorts, and when these Berk-SS/WT chimeras were administered the ACE inhibitor, captopril, the Ang-II concentrations were reduced to the level seen in WT controls (Fig. 4d). More interestingly, captopril treated mice had an attenuated number of circulating HSC/P, compared to vehicle-treated Berk-SS/WT chimeric mice (Fig. 4e). Mechanistically, similarly to our experiments in pharmacological or genetic models of hyperangiotensinemia, we analyzed whether the deficiency of microenvironment AT_2R had any effect on the mobilization of HSC/P in Berk-

SS chimeric mice. Berk-SS BM was transplanted into fully myeloablated WT or $AT_2R^{-/-}$ mice to generate chimeric animals (Supplementary Figs. 5e). All chimeric Berk-SS mice were anemic and showed all the hematological characteristics of primary Berk-SS mice by 6 weeks post-transplantation. Exogenous administration of Ang-II maintained its HSC/P mobilizing effect in Berk-SS/WT chimeric mice, but not in chimeric *Berk-SS/*$AT_2R^{-/-}$ mice (Supplementary Figs.5f), confirming the requirement of AT_2R expression for Ang-II dependent mobilization in SCD mice.

In order to ensure the phenomenon seen in sickle mice also occurs in humans with SCD, we analyzed the levels of Ang-II and the counts of circulating HSC/P in SCD patients and then compared them to unaffected sibling controls with both normal β-globin alleles. All plasma Ang-II levels (Fig. 4f), circulating numbers of $CD34^+$ cells (Fig. 4g) and CFU-C in PB (Fig. 4h) were increased in SCD patients, and treatment with another ACE inhibitor, Lisinopril, resulted in significantly decreased plasma levels of Ang-II and was associated with a corresponding 50–70% reduction in the circulating blood progenitors (Fig. 4f–h).

Discussion

Following a step-by-step approach and combining genetic and pharmacological methods, our manuscript provides a set of compelling data demonstrating the role of high levels of plasma Ang-II in HSC/P mobilization. Mice with chronic hyperangiotensinemia secondary to vasculopathy have a 2–3-fold increase in the number of circulating myeloid committed hematopoietic progenitors and repopulating stem cells. The increase in circulating HSC/P accounts for ~0.1% CRU and ~0.5% CFU-C, respectively, of all BM HSC/P. These levels are similar to the mobilization with the CXCR4 inhibitor, AMD3100[15]. Using combinations of AT receptor KO mice and pharmacological inhibitors, our data support a distinct role for AT2R in BMEC actin polymerization which would coordinate with decreased cortical polymerized actin in HSC/P through either AT1R or AT2R. Ang-II would trigger distinct signaling pathways in HSC/P and BMEC though resulting in a similar outcome, which is the downregulation of activated membrane β1-integrin and HSC/P de-adhesion of HSC/P from their attachment to BMEC. The effect of Ang-II on microenvironmental cells seems to be quite specific since Ang-II does not modify HSC/P adhesion to other cell types such as BM mesenchymal lineage cells.

The translational implications of this work are self-evident. Every year, millions of patients receive anti-angiotensin therapies due to the harmful effects associated with chronic hyperangiotensinemia in cardiac, renal or liver failure. While the ultimate fate of circulating HSC/P remains incompletely understood, there is an abundance of information on their role in innate immune regulation and tissue regeneration. Circulating HSC/P can survey peripheral organs and foster the local production of tissue-resident innate immune cells under steady-state conditions and in response to inflammatory signals[49–51]. An example of hematological vasculopathy is SCD, where vascular occlusions and pathology are a common feature[10]. In these patients, an increased circulatory count of primitive HSC/P in SCD patients is well documented[11] in the context of sustained leukocytosis, which remains a major cause of inflammation associated morbi-mortality[10,52–54]. The absence of a relationship between NO levels and Ang-II dependent HSC/P mobilization suggests that

hyperangiotensinemia together with NO acting on HSC release from endothelial niches[36], may act to mobilize HSC/P via different pathways dependent on cell context and induce divergent signaling pathways.

The effects of Ang-II on cytoskeletal dysregulation of HSC/P and BMEC seem to be independently causative of HSC/P mobilization. Other possible effects of hyperangiotensinemia were found not responsible for the mobilizer effect of Ang-II. Increased vascular tone and modulation of nitric oxide levels are known effects of hyperangiotensinemia[27,34]. However, our data rule out the vasopressor or NO mediator effect as mechanisms responsible for Ang-II dependent HSC/P mobilization. β-adrenergic stimulation has also been shown to be critical at controlling HSC/P egress [24]. We did not observe any significant changes in the levels of norepinephrine or epinephrine in the BM or blood of mice with chronic hyperangiotensinemia, nor did the β-adrenergic blocker propranolol have an effect on their circulating HSC/P counts, suggesting that in the context of vasculopathy, sympathetic nervous system blockade may not counteract the effect of Ang-II.

Our data indicate that hyperangiotensinemia induces HSC/P de-adhesion and mobilization through a direct effect on AT receptors in a cell autonomous and non-cell autonomous fashion. HSC/P mobilization depends on the expression of AT_2R in the endothelium, but not in the mesenchymal stroma of the BM microenvironment. Ang-II signals through BMEC AT_2R, and through both AT_1R and AT_2R in HSC/P, resulting in distinct changes in RhoA activation and in cytoskeletal rearrangements of both BMEC and HSC/P, which result in common downregulation of the levels of active membrane β1-integrin, HSC/P de-adhesion and mobilization (Figure 5). Gene deletion of *RhoA* phenocopies the mobilization effect of Ang-II, and RhoA-deficient mice become insensitive to Ang-II, suggesting that RhoA activation is indispensable for Ang-II dependent mobilization.

Altogether, this data indicates that hyperangiotensinemia/AT_2R signaling plays a homeostatic role in the control of the number of circulating progenitors in vasculopathies in general, and in SCD in particular. These studies demonstrate that acute or chronic hyperangiotensinemia results in HSC/P mobilization and represents a common pathway controlling HSC/P traffic in disease. Targeting Ang-II generation in vasculopathies and SCD may have a detrimental effect on the regenerative roles of circulating stem cells and progenitors, which, clinicians should take into account when using anti-angiotensin therapies.

METHODS

Animals

All animals were treated in accordance with the National Institutes of Health Guide for the Care and Use of Laboratory Animals and all protocols were approved by institutional care and use committees for animal research at the Cincinnati Children's Hospital Research Foundation. Endothelial specific-*Cx43* deficient mice were generated by crossing Tek promoter-Cre recombinase transgenic mice with biallelic Cx43 floxed mice[55]. *Mx1Cre; RhoA$^{flox/flox}$* mice [56] were used, in which inactivation of RhoA in the whole BM as well as

hematopoietic cells was induced by intraperitoneal administration of double-stranded RNA polyI:C (Amersham pharmacia Biotech, Germany) at a dose of 10 mgperKg, every other day for 2 doses. These mice had been backcrossed for a minimum of 5 generations.

AT_1Ra (AT_1R) knockout mice[57] were obtained from Jackson Labs. AT_2R knockout mice [58] were kindly provided by Dr. Inagami (Vanderbilt University School of Medicine, Nashville, TN). *TekCre;Cx43$^{flox/flox}$; AT$_2$R$^{-/-}$* mice and their genetic littermate controls were generated by crossing *TekCre;Cx43$^{flox/flox}$* mice with AT_2R knockout mice. Ubiquitin C-EGFP mice have been generated previously [59]. These mice had been backcrossed >10 generations into C57Bl/6 mice. Berk-SS mice[48] were backcrossed for four generations into C57Bl/6 background to allow survival through adulthood. Experimental transgenic animals were male or female with ages ranging from 6 to 20 weeks. Six to eight week-old female WT C57Bl/6 mice were obtained commercially (Jackson Laboratory, Bar Harbor, ME; Harlan Laboratories, Frederick, MD) and used as WT donors and/or recipients of transduction-transplantation models.

Human specimens

PB specimens from healthy normal volunteers were obtained through Institutional Review Board-approved protocols and donor informed consents from Cincinnati Children's Hospital Medical Center and the University of Cincinnati. PB specimens from unaffected siblings with no sickle cell trait or SCD in different phase (age ≥ 6 years of age) were collected through Institutional Review Board-approved protocols and donor informed consent from Cincinnati Children's Hospital Medical Center and the University of Cincinnati.

Flow Cytometry Analysis and Sorting

For the phonotypical characterization of HSC/P, LDBM cells were obtained after separation using Histopaque-1083 (Sigma, Saint Louis, MO) and stained with allophycocyanin-cyanan7 (APC-Cy7)-conjugated lineage markers (CD45R (B220; clone RA3-6B2), Gr-1 (Ly-6G and Ly-6C; clone RB6-8C5), CD4 (L3T4; clone RM4-5), CD8a (Ly-2; clone 53-6.7), CD3e (clone 145-2C11), CD11b (M1/70), and Ter119 (Ly-76), allophycocyanin (APC)-conjugated c-Kit and FITC conjugated Sca-1 antibodies to identify the Lin^-/c-kit^+/ Sca-1^+ (LSK) BM cell population. IL7Rα (PE Cy7 conjugated, clone SB/199), CD34 (Pacific blue, clone RAM34), CD16/CD32 (PerCp-Cy5.5 conjugated, clone 2.4G2) and CD135 (PE-conjugated, clone A2F10) were used. A sequential gating strategy on nucleated cells as discriminated by light scatter properties and sequencial gating of lineage negative, c-kit+/Sca-1+ (LSK) or c-kit+/Sca-1 (LK) was used. For additional subpopulations, LT-HSC were defined as LSK/CD34−/CD135−; ST-HSC were defined as LSK/CD34+/CD135− and MPP were defined as LSK/CD34+/CD135+. For more differentiated progenitors, MEP were defined as LK/CD34−/CD16/CD32−; CMP were defined as LK/CD34+/CD16/CD32− and GMP were defined as LK/CD34+/CD16/CD32+ events. For sorting of BM derived EC, PE conjugated CD45 and Ter119 antibodies were used along with APC conjucated CD31 (clone MEC 13.3) and FITC conjugated CD106 (clone 429) and sorted by flow cytometry (FACSAria II, BD Biosciences, San Jose CA). Rhodamine phalloidin (Invitrogen), PE-conjugated β1-integrin (eBioHMb1-1) or CD62E (clone 10E9.6), FITC conjugated VCAM-1 (CD106, clone 429) were used and compared to isotype controls to analyze

expressions of adhesion molecules in BMEC cells or sorted LK BM cells. LK or BMEC cells were treated with primary antibody against the membrane bound active form of β1 integrin (9EG7) followed by Alexa-Fluor 647 conjugated goat anti-Rat IgG. The mean fluorescence intensity (MFI) was normalized to that of the isotype control as a ratio.

Competitive repopulation and CFU-C

For the analysis of CRU in PB or BM, 200–400 μL of PB or 3×10^6 BM were transplanted together with 3×10^6 CD45.1$^+$ BM B6.SJL$^{Ptprca\ Pepcb/BoyJ}$ (CD45.1$^+$) into CD45.1$^+$ mice. Hematopoietic cell engraftment was examined by CD45.1 and CD45.2 determination using flow cytometry analysis and analyzed at 4 months post-transplantation. Frequencies of circulating hematopoietic progenitors in PB or BM were analyzed after 9 days of methylcellulose culture (Stem Cell Technologies). Peripheral blood total and differential counts were analyzed using a Hemavet 950 (DREW Scientific).

In vivo drug administration

All inhibitors and antagonists were given by intraperitoneal injection. Ang-II (Sigma Aldrich, 1.44 mg per kg) and enalapril (Sigma Aldrich, 1 mg per kg) were dissolved in PBS[60]. PBS dissolved L-NAME (Sigma Aldrich, 10 mg per kg) was injected and PB was drawn at 10 minutes post-administration [61]. Acidic deoxygenated buffer dissolved SNAP (Cayman, Ann Arbor, MI) was diluted in PBS (20 μg per kg) and PB was collected after 20 minutes of injection [62]. Propranolol was dissolved in water (Sigma Aldrich, 10 mg per kg) then administrated to mice intraperitoneally and PB was collected after 20 minutes of injection[63]. Losartan was administered intraperitoneally (Northstar Rx LLC, Memphis, TN, 50 mg per Kg)[64] two hours before administration of PBS or Ang-II. Captopril (Wockhardt USA LLC, Parsippany, NJ) was mixed with drinking water (0.15 mg per mL for captopril) and given ad libitum in bottles that were changed twice a week. SS chimeric mice were treated with captopril for 10 weeks. Compound 21 (C21, Vicore Pharma, Sweden) was injected i.p. (4 mg per kg) to mice and PB was drawn post 4 hours of C21 administration for analysis. 0.2 mg/kg G-CSF (Neupogen, Amgen Inc, Thousand Oaks, CA) was daily injected intraperitoneally for 5 days. Two different doses of hydralazine (1 mg per kg and 5 mg per kg, Sigma-aldrich) were intravenously administered with similar results and Ang-II injection was followed after 45 minutes post hydralazine administration[26]. For a continuous infusion of Ang-II *in vivo*, osmo pump (alzet mini-osmotic pump, DURECT Corporation, Cupertino, CA) surgery was performed. To reach the similar plasma Ang-II concentration as one bolus of i.p. injection, the pumps were filled with Ang-II (14 μg per mL) or PBS as vehicle control. The Osmo pumps were subcutaneously placed on the back of the mice and the mice were monitored for a week to check the plasma concentration of Ang-II and HSC/P contents in PB.

HSC/P adhesion

EC cells from BM of WT or HyperAng-II$^{\Delta Cx43\text{-}EC}$ mice were isolated from whole BM using FACS sorting (CD45$^-$/Ter119$^-$/CD31$^+$/CD106$^+$) then cultured in endothelial cell growth medium-2 (EGM™-2, Lonza, Walkersville, MD) until freshly confluent on 24 well-plates. Stromal cells from HyperAng-II$^{\Delta Cx43\text{-}EC}$ mice were also purified and expanded as

previously published by our group [22] and used in these assays. WT LDBM cells were harvested from C57Bl/6 mice and 100,000 cells were plated onto EC or stromal cells in triplicate and let adhere for 1 hour. After adhesion, cocultures were treated with vehicle or 100 μM Ang-II for 15 minutes. The supernatant was removed and washed gently twice. Adhesion of BM WT HSC/P was quantified using a CFU-C assay.

ELISA tests

PB was collected in tubes containing EDTA and centrifuged at 3000 × *g* for 20 minutes at 4°C for immediate separation of plasma. To prevent degradation of Ang-II, an inhibitor cocktail was added and the solution stored at −80°C until used for the ELISA assay. Phenyl cartridge columns (ALPCO, NH) were used to extract highly purified Ang-II from the plasma. The cross-reactivity with other forms of angiotensin is comparatively low (Angiotensin I, 4%; Angiotensin 1–7, <0.001%). The concentration of Ang-II from PB was calculated according to manufacturer's protocol (Cayman). Total nitrite and nitrate concentration were measured using freshly drawn PB from the mice, according to manufacturer's protocol (R&D systems). Soluble Cxcl12 and Scf were measured in the extracellular fluid of femoral BM as previously described by our group[22]. The concentrations of norepinephrine and epinephrine in plasma as well as in femoral BM were measured according to manufacturer's protocol (Labor Diagnostika Nord GmbH & Co.KG).

Western blotting and pull-down assays

Lineage negative cells were purified using magnetic bead based methods (Miltenyi biotec) and protein extracts were prepared using a radioimmunoprecipitation lysis buffer (RIPA, Cell Signaling Technology, Danvers, MA) or for pull-down assays, a high-Mg^{++} containing buffer supplemented with protease and phosphatases inhibitor cocktails following manufacturer's instructions (Roche Applied Science, Mannheim, Germany). GTPase activities as well as protein expression and phosphorylation were measured as previously described by our group[39] by effector binding precipitation with p21-activated kinase-bound beads (for Rac activity), and rhotekin-bound beads (for Rho activity) (Cell Signaling Technology). The lysates were separated using 10% SDS-PAGE gels, transferred to PVDF membranes and detected with antibodies. The primary antibodies used were; β-actin (1:6000, clone AC-15, Sigma Aldrich), AT_1R (1:1000, clone 1E10-1A9, abcam), AT_2R (1:500, clone EPR3876, abcam). Antibodies against eNOS (polyclonal, 1:1000), phospho-eNOS (1:1000, clone C9C3,), MLC (polyclonal, 1:1000), p-MLC (Ser19, polyclonal, 1:1000), cofilin (1:1000, clone D59) and p-cofillin (1:1000, clone 77G2; Ser3) were obtained from Cell Signaling, Cx43 (1:500, clone CX-1B1, Invitrogen), and Rac (1:2000), Rho (1:1000) and VEGFR2 (1:500) from Millipore. Gels were visualized using autoradiography and band density analyzed (Image J software, National Institutes of Health, USA) at the expected electrophoretic moiety for each protein molecular weight. Complete, uncropped images of Western blots used for figure illustrations are provided in the Supplementary Fig. 6.

Immunofluorescence and confocal microscopy imaging

The confocal images of the BM endothelial cells treated with 10μM angiotensin for different time periods were acquired using LSM 710 (Carl Zeiss) confocal system at 10X optical magnification. The merged images of rhodamine-phalloidin and DAPI are presented. B) At different time point of angiotensin treatment, the cells that have morphological changes with condensation of actin filaments in the cortical region are counted, and presented as percentage of total cells in the field. At least 10 fields for each time point were counted. The diameter (width) of the cells at each time point was measured using ZEN 2010 software equipped with LSM 710 confocal system. The width of all cells in a field (Each field contains around 60–80 cells) were measured, and the average diameter of each field was calculated. For each time point, 8–10 fields of images were measured, and therefore a total of 600–800 cells were measured for the quantification of the diameter of the cells at each time point of angiotensin treatment. Bar=50μm. Sorted LK cells stained with CFSE (1 μM, Invitrogen) or from ubiquitin C-EGFP mice were cocultured with WT BMEC for four hours in absence of other additives and for another additional hour in absence or presence of 100 nM losartan (Northstar Rx LLC, Memphis, TN), 1 μM PD123319 (Tocris Bioscience, Bristol, UK) or both. At the end of the incubation period, Ang-II was added for 5 minutes, before any significant HSC/P detachment occurs, and cultures were fixed with 4% formaldehyde. The stained cells were analyzed by a LSM 510 confocal system (Carl Zeiss) equipped with an inverted microscope (Observer Z1, Carl Zeiss) using a Plan Apochromat 63X 1.4 NA oil immersion lens. Argon ion 488, HeNe 543, and HeNe633 laser lines were used to excite EGFP, rhodamine and Topro3, respectively. The acquired images were 3-D reconstituted, then the phalloidin-rhodamine staining on LK cells was isolated by electronically removing the phalloidin-rhodamine staining of EC (IMARIS BITPLANE software), and processed using Adobe Photoshop v7.

Statistical Analysis

Quantitative data is given as mean ± standard error of the mean (SEM). Statistical significance was determined using an unpaired Student-t test or one-way Anova with Bonferroni correction. A value of $p < 0.05$ was considered to be statistically significant.

Supplementary Material

Refer to Web version on PubMed Central for supplementary material.

Acknowledgments

We thank Dr. Hartmut Geiger (University of Ulm) for helpful comments and Ms. Margaret O'Leary for editing the manuscript. We also thank Jeff Bailey and Victoria Summey for technical assistance and the Mouse and Research Flow Cytometry Core Facilities, both supported by National Institutes of Health/Centers of Excellence for Molecular Hematology Grant 1P30DK090971-01. We also want to thank the Hematology Repository for human specimens from sickle cell anemia patients and controls. This project was funded by the Heimlich Institute of Cincinnati (J.A.C.), U.S. Department of Defense #10580355 (J.A.C.), National Institutes of Health/NHLBI R01-HL087159 and HL087159S1 (J.A.C.), U01-HL117709 and R34-HL108752 (P.M.); R01 AG040118, R01 CA141341 and R01 CA150547 (Y.Z.); the Center for Clinical Translational Science and Training Awards (J.A.C & P.M.) and National Blood Foundation (K.H.C.) and funds from the Hoxworth Blood Center and Cincinnati Children's Hospital Medical Center (to J.A.C.).

References

1. Hoggatt J, et al. Differential stem- and progenitor-cell trafficking by prostaglandin E2. Nature. 2013; 495:365–369. [PubMed: 23485965]
2. Greenbaum A, et al. CXCL12 in early mesenchymal progenitors is required for haematopoietic stem-cell maintenance. Nature. 2013; 495:227–230. [PubMed: 23434756]
3. Ding L, Saunders TL, Enikolopov G, Morrison SJ. Endothelial and perivascular cells maintain haematopoietic stem cells. Nature. 2012; 481:457–462. [PubMed: 22281595]
4. Mendez-Ferrer S, Lucas D, Battista M, Frenette PS. Haematopoietic stem cell release is regulated by circadian oscillations. Nature. 2008; 452:442–447. [PubMed: 18256599]
5. Casanova-Acebes M, et al. Rhythmic modulation of the hematopoietic niche through neutrophil clearance. Cell. 2013; 153:1025–1035. [PubMed: 23706740]
6. Ghanem LY, et al. Hematopoietic stem cell mobilization into the peripheral circulation in patients with chronic liver diseases. Journal of digestive diseases. 2012; 13:571–578. [PubMed: 23107444]
7. Hohenstein B, et al. Enhanced progenitor cell recruitment and endothelial repair after selective endothelial injury of the mouse kidney. American journal of physiology Renal physiology. 2010; 298:F1504–1514. [PubMed: 20237239]
8. Valgimigli M, et al. CD34+ and endothelial progenitor cells in patients with various degrees of congestive heart failure. Circulation. 2004; 110:1209–1212. [PubMed: 15249502]
9. Korbling M, Estrov Z, Champlin R. Adult stem cells and tissue repair. Bone Marrow Transplant. 2003; 32 (Suppl 1):S23–24. [PubMed: 12931235]
10. Telen MJ. Role of adhesion molecules and vascular endothelium in the pathogenesis of sickle cell disease. Blood (Education Program of the American Society of Hematology). 2007:84–90.
11. Croizat H, Ponchio L, Nicolini FE, Nagel RL, Eaves CJ. Primitive haematopoietic progenitors in the blood of patients with sickle cell disease appear to be endogenously mobilized. Br J Haematol. 2000; 111:491–497. [PubMed: 11122089]
12. Sayer G, Bhat G. The renin-angiotensin-aldosterone system and heart failure. Cardiol Clin. 2014; 32:21–32. vii. [PubMed: 24286576]
13. Group CT. COSSACS (Continue or Stop post-Stroke Antihypertensives Collaborative Study): rationale and design. J Hypertens. 2005; 23:455–458. [PubMed: 15662235]
14. Griffing GT, Melby JC. Enalapril (MK-421) and the white cell count and haematocrit. Lancet. 1982; 1:1361. [PubMed: 6123665]
15. Vlahakos DV, Canzanello VJ, Madaio MP, Madias NE. Enalapril-associated anemia in renal transplant recipients treated for hypertension. Am J Kidney Dis. 1991; 17:199–205. [PubMed: 1992663]
16. Gould AB, Goodman SA. Effect of an angiotensin-converting enzyme inhibitor on blood pressure and erythropoiesis in rats. Eur J Pharmacol. 1990; 181:225–234. [PubMed: 2143478]
17. Dahlof B, et al. Cardiovascular morbidity and mortality in the Losartan Intervention For Endpoint reduction in hypertension study (LIFE): a randomised trial against atenolol. Lancet. 2002; 359:995–1003. [PubMed: 11937178]
18. Julius S, et al. Outcomes in hypertensive patients at high cardiovascular risk treated with regimens based on valsartan or amlodipine: the VALUE randomised trial. Lancet. 2004; 363:2022–2031. [PubMed: 15207952]
19. Vlahakos DV, Marathias KP, Madias NE. The role of the renin-angiotensin system in the regulation of erythropoiesis. Am J Kidney Dis. 2010; 56:558–565. [PubMed: 20400218]
20. Liao Y, Day KH, Damon DN, Duling BR. Endothelial cell-specific knockout of connexin 43 causes hypotension and bradycardia in mice. Proc Natl Acad Sci USA. 2001; 98:9989–9994. [PubMed: 11481448]
21. Broxmeyer HE, et al. Rapid mobilization of murine and human hematopoietic stem and progenitor cells with AMD3100, a CXCR4 antagonist. J Exp Med. 2005; 201:1307–1318. [PubMed: 15837815]

22. Gonzalez-Nieto D, et al. Connexin-43 in the osteogenic BM niche regulates its cellular composition and the bidirectional traffic of hematopoietic stem cells and progenitors. Blood. 2012; 119:5144–5154. [PubMed: 22498741]
23. Taniguchi Ishikawa E, et al. Connexin-43 prevents hematopoietic stem cell senescence through transfer of reactive oxygen species to bone marrow stromal cells. Proc Natl Acad Sci USA. 2012; 109:9071–9076. [PubMed: 22611193]
24. Katayama Y, et al. Signals from the sympathetic nervous system regulate hematopoietic stem cell egress from bone marrow. Cell. 2006; 124:407–421. [PubMed: 16439213]
25. Berk BC. Angiotensin type 2 receptor (AT2R): a challenging twin. Science STKE. 2003; 2003:PE16.
26. Horsman MR, Christensen KL, Overgaard J. Relationship between the hydralazine-induced changes in murine tumor blood supply and mouse blood pressure. Int J Rad Oncol Biol Phys. 1992; 22:455–458.
27. Qi G, et al. Angiotensin II infusion-induced inflammation, monocytic fibroblast precursor infiltration, and cardiac fibrosis are pressure dependent. Cardiovasc Toxicol. 2011; 11:157–167. [PubMed: 21373977]
28. Khayyal M, Gross F, Kreye VA. Studies on the direct vasodilator effect of hydralazine in the isolated rabbit renal artery. J Pharmacol Exp Ther. 1981; 216:390–394. [PubMed: 7463355]
29. Burson JM, Aguilera G, Gross KW, Sigmund CD. Differential expression of angiotensin receptor 1A and 1B in mouse. Am J Physiol. 1994; 267:E260–267. [PubMed: 8074205]
30. Kaschina E, et al. Angiotensin II type 2 receptor stimulation: a novel option of therapeutic interference with the renin-angiotensin system in myocardial infarction? Circulation. 2008; 118:2523–2532. [PubMed: 19029468]
31. Steckelings UM, et al. Non-peptide AT2-receptor agonists. Curr Op Pharmacol. 2011; 11:187–192.
32. Cancelas JA, et al. Rac GTPases differentially integrate signals regulating hematopoietic stem cell localization. Nat Med. 2005; 11:886–891. [PubMed: 16025125]
33. Milsom MD, Lee AW, Zheng Y, Cancelas JA. Fanca−/− hematopoietic stem cells demonstrate a mobilization defect which can be overcome by administration of the Rac inhibitor NSC23766. Haematologica. 2009; 94:1011–1015. [PubMed: 19491337]
34. Olson S, et al. Angiotensin II stimulates nitric oxide production in pulmonary artery endothelium via the type 2 receptor. Am J Physiol. 2004; 287:L559–568.
35. Landmesser U, Drexler H. The clinical significance of endothelial dysfunction. Curr Op Cardiol. 2005; 20:547–551.
36. Aicher A, Heeschen C, Dimmeler S. The role of NOS3 in stem cell mobilization. Trends Mol Med. 2004; 10:421–425. [PubMed: 15350893]
37. Sugiyama T, Kohara H, Noda M, Nagasawa T. Maintenance of the hematopoietic stem cell pool by CXCL12-CXCR4 chemokine signaling in bone marrow stromal cell niches. Immunity. 2006; 25:977–988. [PubMed: 17174120]
38. Papayannopoulou T, Craddock C, Nakamoto B, Priestley GV, Wolf NS. The VLA4/VCAM-1 adhesion pathway defines contrasting mechanisms of lodgement of transplanted murine hemopoietic progenitors between bone marrow and spleen. Proc Natl Acad Sci USA. 1995; 92:9647–9651. [PubMed: 7568190]
39. Winkler IG, et al. Vascular niche E-selectin regulates hematopoietic stem cell dormancy, self renewal and chemoresistance. Nat Med. 2012; 18:1651–1657. [PubMed: 23086476]
40. Jiang B, Xu S, Hou X, Pimentel DR, Cohen RA. Angiotensin II differentially regulates interleukin-1-beta-inducible NO synthase (iNOS) and vascular cell adhesion molecule-1 (VCAM-1) expression: role of p38 MAPK. J Biol Chem. 2004; 279:20363–20368. [PubMed: 15001568]
41. Guilluy C, et al. The Rho exchange factor Arhgef1 mediates the effects of angiotensin II on vascular tone and blood pressure. Nat Med. 2010; 16:183–190. [PubMed: 20098430]
42. Loirand G, Pacaud P. The role of Rho protein signaling in hypertension. Nat Rev Cardiol. 2010; 7:637–647. [PubMed: 20808285]
43. Cortez-Retamozo V, et al. Angiotensin II drives the production of tumor-promoting macrophages. Immunity. 2013; 38:296–308. [PubMed: 23333075]

44. Daley WP, Kohn JM, Larsen M. A focal adhesion protein-based mechanochemical checkpoint regulates cleft progression during branching morphogenesis. Dev Dyn. 2011; 240:2069–2083. [PubMed: 22016182]
45. Taniguchi Ishikawa E, et al. Klf5 controls bone marrow homing of stem cells and progenitors through Rab5-mediated beta1/beta2-integrin trafficking. Nat Comm. 2013; 4:1660.
46. Bolomini-Vittori M, et al. Regulation of conformer-specific activation of the integrin LFA-1 by a chemokine-triggered Rho signaling module. Nat Immunol. 2009; 10:185–194. [PubMed: 19136961]
47. Palamidessi A, et al. Endocytic trafficking of Rac is required for the spatial restriction of signaling in cell migration. Cell. 2008; 134:135–147. [PubMed: 18614017]
48. Paszty C, et al. Transgenic knockout mice with exclusively human sickle hemoglobin and sickle cell disease. Science. 1997; 278:876–878. [PubMed: 9346488]
49. Baldridge MT, King KY, Boles NC, Weksberg DC, Goodell MA. Quiescent haematopoietic stem cells are activated by IFN-gamma in response to chronic infection. Nature. 2010; 465:793–797. [PubMed: 20535209]
50. Essers MA, et al. IFNalpha activates dormant haematopoietic stem cells in vivo. Nature. 2009; 458:904–908. [PubMed: 19212321]
51. Massberg S, et al. Immunosurveillance by hematopoietic progenitor cells trafficking through blood, lymph, and peripheral tissues. Cell. 2007; 131:994–1008. [PubMed: 18045540]
52. Wun T. The Role of Inflammation and Leukocytes in the Pathogenesis of Sickle Cell Disease; Haemoglobinopathy. Hematology. 2001; 5:403–412. [PubMed: 11399640]
53. Hebbel RP, Osarogiagbon R, Kaul D. The endothelial biology of sickle cell disease: inflammation and a chronic vasculopathy. Microcirculation. 2004; 11:129–151. [PubMed: 15280088]
54. Wood KC, Hsu LL, Gladwin MT. Sickle cell disease vasculopathy: a state of nitric oxide resistance. Free radical biology & medicine. 2008; 44:1506–1528. [PubMed: 18261470]
55. Gutstein DE, et al. Conduction slowing and sudden arrhythmic death in mice with cardiac-restricted inactivation of connexin43. Circ Res. 2001; 88:333–339. [PubMed: 11179202]
56. Zhou X, et al. RhoA GTPase Controls Cytokinesis and Programmed Necrosis of Hematopoietic Progenitors. J Exp Med. 2013; 210:2371–85. [PubMed: 24101377]
57. Ito M, et al. Regulation of blood pressure by the type 1A angiotensin II receptor gene. Proc Natl Acad Sci USA. 1995; 92:3521–3525. [PubMed: 7724593]
58. Hein L, Barsh GS, Pratt RE, Dzau VJ, Kobilka BK. Behavioural and cardiovascular effects of disrupting the angiotensin II type-2 receptor in mice. Nature. 1995; 377:744–747. [PubMed: 7477266]
59. Schaefer BC, Schaefer ML, Kappler JW, Marrack P, Kedl RM. Observation of antigen-dependent CD8+ T-cell/dendritic cell interactions in vivo. Cell Immunol. 2001; 214:110–122. [PubMed: 12088410]
60. Sakamoto K, Sugimoto K, Sudoh T, Fujimura A. Different effects of imidapril and enalapril on aminopeptidase P activity in the mouse trachea. Hypert Res. 2005; 28:243–247.
61. Calignano A, Persico P, Mancuso F, Sorrentino L. L-arginine modulates morphine-induced changes in locomotion in mice. Ann Istituto Sup Sanita. 1993; 29:409–412.
62. Ito Y, Abril ER, Bethea NW, McCuskey RS. Role of nitric oxide in hepatic microvascular injury elicited by acetaminophen in mice. Am J Physiol Gastrointest Liv Phsyiol. 2004; 286:G60–67.
63. Shih MF, Taberner PV. Selective activation of brown adipocyte hormone-sensitive lipase and cAMP production in the mouse by beta 3-adrenoceptor agonists. Biochem Pharmacol. 1995; 50:601–608. [PubMed: 7669062]
64. Lukawski K, Janowska A, Jakubus T, Tochman-Gawda A, Czuczwar SJ. Angiotensin AT1 receptor antagonists enhance the anticonvulsant action of valproate in the mouse model of maximal electroshock. Eur J Pharmacol. 2010; 640:172–177. [PubMed: 20465998]

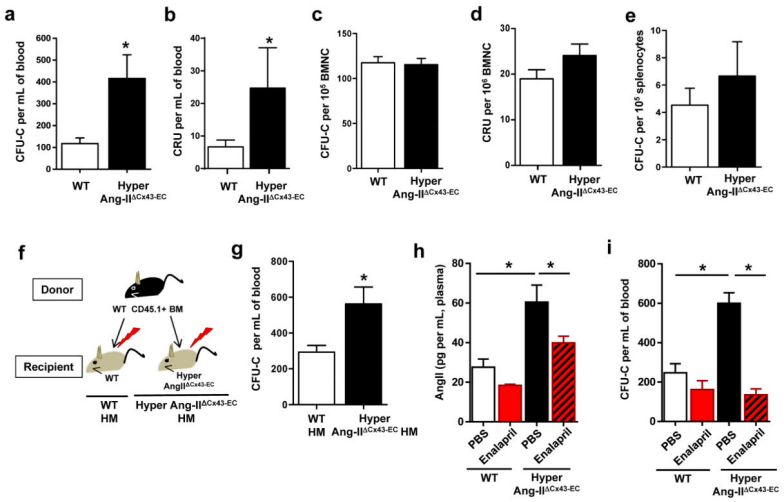

Figure 1. Circulating HSC/P count is increased in chronic hyperangiotensinemia mouse model

(a) Frequency of hematopoietic progenitors in basal conditions of WT (n=10) or HyperAng-II$^{\Delta Cx43\text{-}EC}$ (n= 10) mice. *p<0.05. (b) Competitive repopulating unit frequency (CRU) of stem cells in PB from WT (n=9) or HyperAng-II$^{\Delta Cx43\text{-}EC}$ (n=14) mice. *p<0.05. (c) BM CFU-C content in basal conditions of WT (n=4) or HyperAng-II$^{\Delta Cx43\text{-}EC}$ mice (n=4). (d) Frequency of BM CRU from WT (n=16) or HyperAng-II$^{\Delta Cx43\text{-}EC}$ mice (n= 17) mice. (e) CFU-C in spleen from basal WT (n=3) or HyperAng-II$^{\Delta Cx43\text{-}EC}$ (n=3) mice. (f) Schema of generation of HM chimeras by transplantation of WT BM cells into WT or HyperAng-II$^{\Delta Cx43\text{-}EC}$ mice. (g) Frequency of hematopoietic progenitors in basal conditions of WT HM (n=6) or HyperAng-II$^{\Delta Cx43\text{-}EC}$ HM mice (n= 6) mice. Open bars depict data from WT mice. Solid bars depict data from HyperAng-II$^{\Delta Cx43\text{-}EC}$ mice. (h) Ang-II concentration in plasma and (i) count of PB CFU-C in WT and HyperAng-II$^{\Delta Cx43\text{-}EC}$ mice treated with PBS (open bars; WT, black bars; HyperAng-II$^{\Delta Cx43\text{-}EC}$) or enalapril (red bars; WT, hatched red bars; HyperAng-II$^{\Delta Cx43\text{-}EC}$). Values represent mean ± SEM of 3 independent experiments, with a minimum of 3 mice per group and experiment. *p<0.05, Student's t test for experiments that compare two groups or Anova test with Bonferroni correction for experiments with more than two groups.

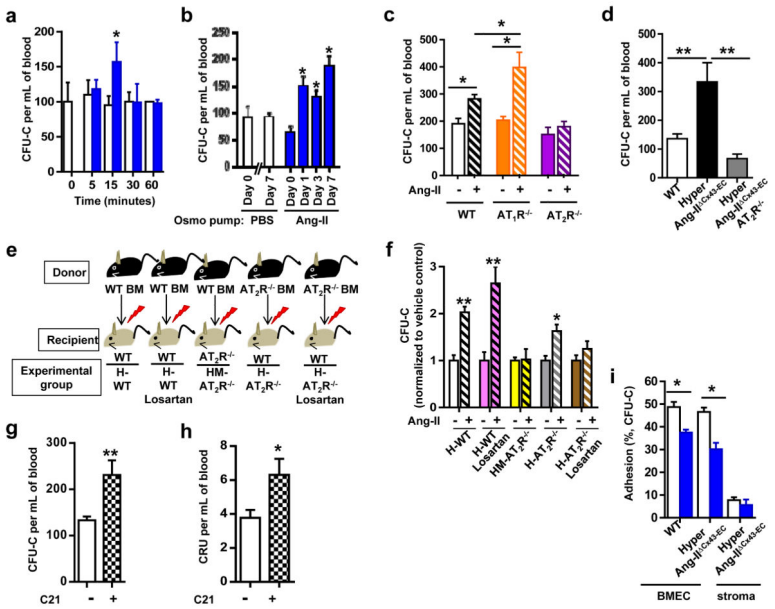

Figure 2. Ang-II induces HSC/P de-adhesion and mobilization through AT_2R signaling

(a) Ang-II time kinetics of HSC/P mobilization. CFU-C of Ang-II injected mice (blue) were compared to vehicle control treated mice (open bars) at each time point. (b) PB CFU-C counts in mice submitted to continuous infusion of Ang-II for up to 7 days. (c) WT (black outlined bars), $AT_1R^{-/-}$ (orange bars) and $AT2R^{-/-}$ (purple bars) primary mice were injected with PBS (−, solid bars) or Ang-II (+, hatched bars). N=4 for each group. (d) CFU-C count in PB from WT, HyperAng-II$^{\Delta Cx43\text{-}EC}$, and AT2R deficient-HyperAng-II$^{\Delta Cx43\text{-}EC}$ mice. (e) Schema of transplantation to generate AT_2R deficient in H- or HM mice. (f) Chimeric mice (H-WT, empty bars; H-WT pretreated with losartan, pink bars; $HM\text{-}AT_2R^{-/-}$, yellow bars; $H\text{-}AT_2R^{-/-}$, grey bars; $H\text{-}AT_2R^{-/-}$ pretreated with losartan, brown bars) were injected with PBS (−, solid bars) or Ang-II (+, hatched bars). The CFU-C counts were normalized to vehicle control (−, PBS). (g–h) Circulating CFU-C and CRU in PB from mice administered vehicle control (−, PBS, open bar) or C21 (4 mg per Kg b.w., mosaic bar). (g) CFU-C counts. Values represent mean ± SEM of 3 independent experiments with a minimum of 12 mice per group. (h) CRU counts; N=7 mice per group. (i) Adhesion of WT hematopoietic progenitors to EC from WT or HyperAng-II$^{\Delta Cx43\text{-}EC}$ mice. BM stromal cells from HyperAng-II$^{\Delta Cx43\text{-}EC}$ mice were used as a negative control. EC or stromal cells were treated with 100 μM Ang-II and the percentage of adhesion (blue bars) was compared to the adhesion of vehicle treated cells (open bars). *p<0.05; ** p<0.01, Student's t test for experiments that compare two groups or Anova test with Bonferroni correction for experiments with more than two groups.

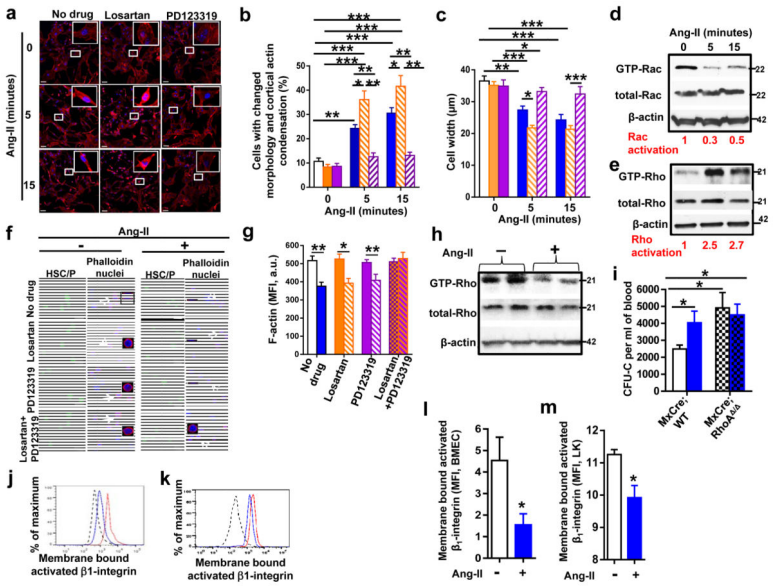

Figure 3. Ang-II alters Rho GTPase family activity and expression of activated β1-integrin

(a) Representative confocal microscopic image of F-actin (phalloidin, red) and nuclear (DAPI, blue) staining of 10 μM Ang-II treated BMEC at different time points. BMEC were pretreated with 100 nM losartan or 1 μM PD123319 or vehicle control for 1 hour before Ang-II exposure. Scale bar = 50 μm. (b) Measurement of morphological changes with cortical actin condensation in BMEC with exposure of vehicle control (open; no drug treated, orange; losartan, and purple; PD123319) or Ang-II (blue; no drug, hatched orange; losartan, and hatched purple; PD123319) in different time points as shown in Fig. 3a. (c) The diameter of all cells (cell width) was measured, and the average diameter of each field was calculated in Fig. 3b. (d–e) Representative immunoblot of effector binding domain pull-down assay for Rac (d) or Rho A (e) in BMEC with different time of Ang-II exposure.(f) Representative confocal microscopic image of F-actin (phalloidin, red) and nuclear (DAPI, blue) staining of LK after 5 minutes exposure of 10 μM Ang-II (+). Ang-II Scale bar = 10 μm. (g) MFI of phalloidin-rhodamine in LK treated with vehicle control (solid bars) or Ang-II (hatched bars) was measured in Fig. 3f. Losartan (100 nM, orange); PD123319 (1 μM, purple); combined losartan and PD123319 (orange/purple mosaic). (h) Representative immunoblot of effector binding domain pull-down assay for Rho A in LK cells with or without Ang-II treatment for 5 minutes. (i) CFU-C counts in PB from polyI:C treated *MxCre; WT* (solid) and *RhoA*$^{flox/flox}$ (mosaic) mice treated with Ang-II (blue) or vehicle control (PBS, black outlined). Data represent mean ± SEM. A minimum of 5 mice were analyzed per group. (j–k) Representative FACS histogram of membrane bound activated membrane β1-integrin in BMEC (j) or LK (k) cells treated with vehicle control (red) or Ang-II (blue) and compared to isotype treated cells (dotted line). (l–m) MFI of membrane bound activated membrane β1-integrin in BMEC (l) or LK (m) treated with vehicle control (open) or Ang-II (blue) was measured in Fig. 2j–k. All experiments were performed minimum of 3 independently. *p<0.05; **p<0.01; ***p<0.001; Student's t test for experiments that compare two groups or Anova test with Bonferroni correction for experiments with more than two groups. For immunoblots, molecular weight markers in KDa are presented on the right side.

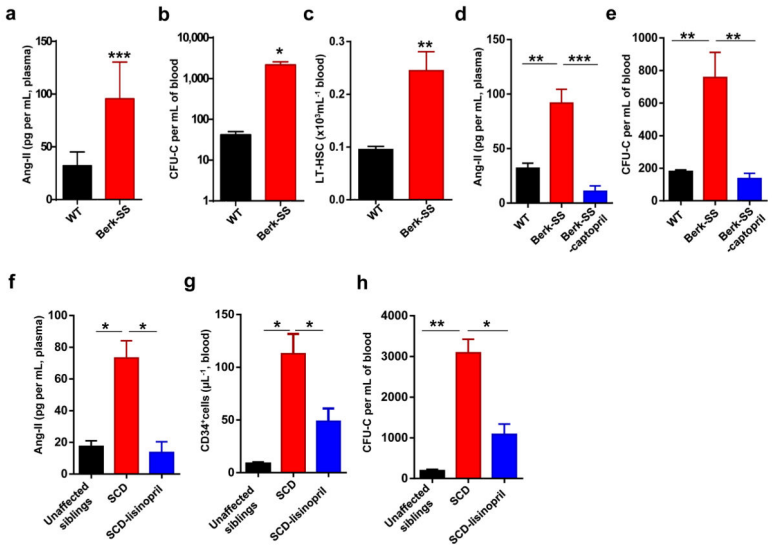

Figure 4. Increased Ang-II level correlates with increased HSC/P circulation in SCD

(a) Plasma Ang-II concentration in Berkeley AA (WT, black) and Berk-SS (red) mice. ***p<0.001. Data represent mean ± SEM. (b) CFU-C in PB from Berkeley AA (WT, black) and Berk-SS (red) mice. (c) LT-HSC in PB from WT and Berk-SS mice. (d) Plasma Ang-II concentration in C57bl/6 mice transplanted with either the BM of AA (WT, black, n=8) or SS mice (red, n=7). Subgroup of chimeric SS mice were treated with captopril (blue, n=7). (e) CFU-C counts in PB from the mice in (c). Data represent mean ± SEM. (f) Ang-II concentration in plasma from age-matched, unaffected sibling control (black, n=8), patient with SCD (red, n=15) and SCD patient with lisinopril treatment (blue, n=4). *p<0.05. Data represent mean ± SEM. (g) Number of circulating $CD34^+$ cells in the PB from (f). Data represent mean ± SEM. (h) CFU-C counts in PB from (g) a healthy age-matched, unaffected sibling controls (black), patients with SCD (red), SCD patients in treatment with lisinopril (blue). Values represent mean ± SEM of 3 independent experiments. * p<0.05. **p<0.01, ***p<0.001, Student's t test for experiments that compare two groups or Anova test with Bonferroni correction for experiments with more than 2 groups.

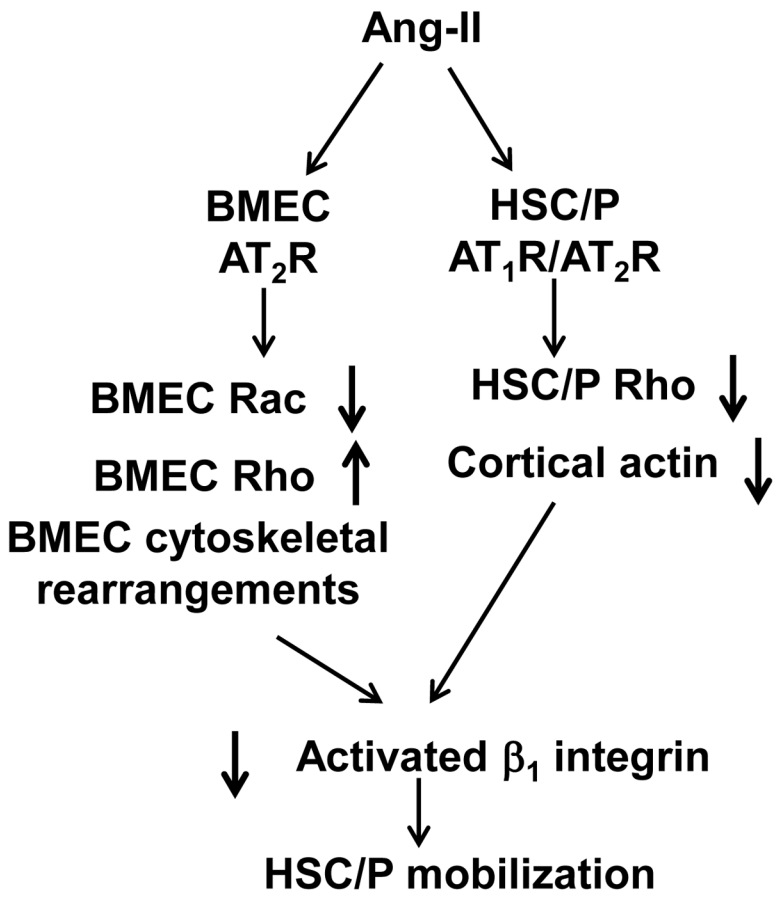

Figure 5. Proposed pathway of Ang-II induced HSC/P mobilization

Upon Ang-II stimulation, AT_2R in EC is mainly responsible for reducing Rac activation and increasing Rho activation resulting in increased actin polymerization and stress fibers. At the same time, cell-autonomous AT1R and AT2R downregulate Rho GTPase activity and actin polymerization in HSC/P resulting in de-adhesion as well. Both mirror images processes of Rho GTPase activation or inhibition result in a common pathway of downregulation of the levels of activated membrane β1-integrin, and consequent detachment of HSC/P from EC.